

**EFFECTS OF THE ECCENTRICITY OF THE PRIMARIES IN THE  
GRAVITATIONAL CAPTURE PHENOMENON**

**Ernesto Vieira Neto**

E-Mail: [ernesto@feg.unesp.br](mailto:ernesto@feg.unesp.br)

Faculdade de Engenharia de Guaratinguetá – UNESP – Guaratinguetá

**Antônio Fernando Bertachini de Almeida Prado**

E-Mail: [prado@dem.inpe.br](mailto:prado@dem.inpe.br)

Instituto Nacional de Pesquisas Espaciais - São José dos Campos - SP - Brazil

Gravitational capture is a characteristic of some dynamical systems in celestial mechanics, as in the elliptic restricted three-body problem that is considered in this paper. The basic idea is that a spacecraft (or any particle with negligible mass) can change a hyperbolic orbit with a small positive energy around a celestial body in an elliptic orbit with a small negative energy without the use of any propulsive system. The force responsible for this modification in the orbit of the spacecraft is the gravitational force of the third body involved in the dynamics. In this way, this force is used as a zero cost control, equivalent to a continuous thrust applied in the spacecraft. One of the most important applications of this property is the construction of trajectories to the Moon. The objective of the present paper is to study in some detail the effects of the eccentricity of the primaries in this maneuver.

**INTRODUCTION**

Gravitational capture is the phenomenon where a particle, coming from outside the sphere of influence of another body, may have its velocity relative to the celestial body reduced and it can even stay in orbit around it temporary, using only gravitational force<sup>1</sup>. This happens due to the change of the two-body energy of the massless body from positive to negative relative to one of the primaries of the restricted three-body problem. The two-body energy is constant in the two-body problem, but not in the three-body problem, where there is no energy conservation due to the perturbation of the third body. The importance of this study is that it can be used to decrease the fuel expenditure

for a mission going from one of the primaries to the other, like an Earth-Moon mission. This is performed by applying an impulse to the spacecraft during the temporary capture to accomplish a permanent capture.

The application of this phenomenon in spacecraft trajectories is recent in the literature. Among the first studies are the ones performed by Belbruno<sup>1-3</sup>; Krish<sup>4</sup>; Krish, Belbruno and Hollister<sup>5</sup>; Miller and Belbruno<sup>6</sup>; Belbruno and Miller<sup>7</sup>. They all studied missions in the Earth-Moon system that use this technique to save fuel during the insertion of the spacecraft in its final orbit around the Moon. Another group of researches that made fundamental contributions in this field, also with the main objective of constructing real trajectories in the Earth-Moon system, are the Japanese Yamakawa, Kawaguchi, Ishii and Matsuo (see references 8 and 9). In particular, Yamakawa wrote his Ph.D. Dissertation<sup>10</sup> in this topic, with several important contributions in this field. A real application of those ideas was made during an emergency in a Japanese spacecraft<sup>11</sup>. After that, some studies that consider the time required for this transfer appeared in the literature. Examples of this approach can be found in the papers by Vieira-Neto and Prado<sup>12,13</sup>.

Some of those references show that the fuel consumption, in a transfer maneuver, can be smaller than the one required by the Hohmann transfer. In this paper we consider this problem under the model given by the elliptic restricted three-body problem. The references that we found related to the gravitational capture for the elliptic case, like Bailey<sup>14,15,16</sup> and Heppenheimer<sup>17</sup> do not use the variation of the two-body energy as we do in this paper.

## **THE ELLIPTIC RESTRICTED THREE-BODY PROBLEM**

The equations of motion for the spacecraft are assumed to be the ones valid for the well-known planar restricted elliptic three-body problem. We also use the standard canonical system of units, which implies that:

1. The unit of distance is the semi-major axis of the orbit  $M_1$  and  $M_2$ ;
2. The angular velocity ( $\omega$ ) of the motion of  $M_1$  and  $M_2$  is assumed to be one;
3. The mass of the smaller primary ( $M_2$ ) is given by  $\mu = \frac{m_2}{m_1 + m_2}$  (where  $m_1$  and  $m_2$  are the real masses of  $M_1$  and  $M_2$ , respectively) and the mass of  $M_2$  is  $(1-\mu)$ , to make the total mass of the system unitary;
4. The unit of time is defined such that the period of the motion of the two primaries is  $2\pi$ ;
5. The gravitational constant is one.

There are several systems that can be used to describe the elliptic restricted problem<sup>18</sup>. In this section the fixed (inertial) and the rotating-pulsating systems are described.

In the fixed system the origin is located in the barycenter of the two heavy masses  $M_1$  and  $M_2$ . The horizontal axis is the line connecting  $M_1$  and  $M_2$  and the vertical axis is perpendicular to the horizontal axis. In this system, the positions of  $M_1$  and  $M_2$  are:

$$\bar{x}_1 = -\mu r \cos v \quad (1)$$

$$\bar{y}_1 = -\mu r \sin v \quad (2)$$

$$\bar{x}_2 = (1-\mu)r \cos v \quad (3)$$

$$\bar{y}_2 = (1-\mu)r \sin v \quad (4)$$

where  $r$  is the distance between the two primaries, given by  $r = \frac{1-e^2}{1+e \cos v}$ , and  $v$  is the true anomaly of  $M_2$ . Then, in this system, the equations of motion of the massless particle are:

$$\bar{x}'' = \frac{-(1-\mu)(\bar{x} - \bar{x}_1)}{r_1^3} - \frac{\mu(\bar{x} - \bar{x}_2)}{r_2^3} \quad (5)$$

$$\bar{y}'' = \frac{-(1-\mu)(\bar{y} - \bar{y}_1)}{r_1^3} - \frac{\mu(\bar{y} - \bar{y}_2)}{r_2^3} \quad (6)$$

where “ $''$ ” means the second derivative with respect to time,  $r_1$  and  $r_2$  are the distances from  $M_1$  and  $M_2$ , given by:

$$r_1^2 = (\bar{x} - \bar{x}_1)^2 + (\bar{y} - \bar{y}_1)^2 \quad (7)$$

$$r_2^2 = (\bar{x} - \bar{x}_2)^2 + (\bar{y} - \bar{y}_2)^2 \quad (8)$$

Now, we will introduce the rotating-pulsating system of reference. In this system, the origin is again the center of mass of the two massive primaries. The horizontal axis ( $x$ ) is the line that connects the two primaries. It rotates with a variable angular velocity in a such way that the two massive primaries are always in this axis. The vertical axis ( $y$ ) is perpendicular to the  $x$  axis. Besides the rotation, the system also pulsates in a such way to keep the massive primaries in fixed positions. To achieve this

situation we have to multiply the unit of distances for the instantaneous value of the distance between the two primaries ( $r$ ). In a system like this one, the positions of the primaries are:

$$x_1 = -\mu, x_2 = 1 - \mu, y_1 = y_2 = 0 \quad (9)$$

In this system, the equations of motion for the massless particle are:

$$\ddot{x} - 2\dot{y} = \frac{r}{p} \left( x - (1 - \mu) \frac{x - x_1}{r_1^3} - \mu \frac{x - x_2}{r_2^3} \right) \quad (10)$$

$$\ddot{y} + 2\dot{x} = \frac{r}{p} \left( y - (1 - \mu) \frac{y}{r_1^3} - \mu \frac{y}{r_2^3} \right) \quad (11)$$

and we also have an equation to relate time and the true anomaly of the primaries:

$$\dot{t} = \frac{r^2}{p^{1/2}} \quad (12)$$

where the overdot means derivative with respect to the true anomaly of the primaries and  $p$  is the semi-latus rectum of the ellipse.

The equations that relate one system to another are:

$$\bar{x} = rx \cos v - ry \sin v \quad (13)$$

$$\bar{y} = rx \sin v + ry \cos v \quad (14)$$

$$x = (\bar{x} \cos v + \bar{y} \sin v) / r \quad (15)$$

$$y = (\bar{y} \cos v - \bar{x} \sin v) / r \quad (16)$$

for the positions and:

$$\bar{x}' = x'r \cos v - y'r \sin v - \frac{x(1 - e^2) \sin v}{(1 + e \cos v)^2} - \frac{y(1 - e^2)(e + \cos v)}{(1 + e \cos v)^2} \quad (17)$$

$$\bar{y}' = x'r \sin v + y'r \cos v - \frac{y(1 - e^2) \sin v}{(1 + e \cos v)^2} + \frac{x(1 - e^2)(e + \cos v)}{(1 + e \cos v)^2} \quad (18)$$

$$x' = \frac{\bar{x}' \cos v}{r} + \frac{\bar{y}' \sin v}{r} - \frac{\bar{x}(\sin v + e \sin 2v)}{1 - e^2} + \frac{\bar{y}(\cos v + 2e \cos^2 v - e)}{1 - e^2} \quad (19)$$

$$y' = \frac{\bar{y}' \cos v}{r} - \frac{\bar{x}' \sin v}{r} - \frac{\bar{y}(\sin v + e \sin 2v)}{1 - e^2} - \frac{\bar{x}(\cos v + 2e \cos^2 v - e)}{1 - e^2} \quad (20)$$

for the velocities, where  $p = 1 - e^2$  and  $r = \frac{1 - e^2}{1 + e \cos v}$ .

## THE GRAVITATIONAL CAPTURE

To define the gravitational capture is necessary to use a few basic concepts from the two-body celestial mechanics. Those concepts are:

- a) Closed orbit: a spacecraft in a orbit around a central body is in a closed orbit if its velocity is not large enough to escape from the central body. It remains always inside a sphere centered in the central body;
- b) Open orbit: a spacecraft in a orbit around a central body is in a open orbit if its velocity is large enough to escape from the central body. In this case, the spacecraft can go to infinity, no matter what is its initial position.

To identify the type of orbit of the spacecraft it is possible to use the definition of the two-body energy (E) of a massless particle orbiting a central body. The equation is  $E = \frac{V^2}{2} - \frac{\mu}{r}$ , where V is the velocity of the spacecraft relative to the central body,  $\mu$  is the gravitational parameter of the central body and r is the distance between the spacecraft and the central body.

With this definition, it is possible to say that the spacecraft is in a open orbit if its energy is positive and that it is in a closed orbit if its energy is negative. In the two-body problem this energy remains constant and it is necessary to apply an external force to change it. This energy is no longer constant in the restricted three-body problem. Then, for some initial conditions, a spacecraft can alternate the sign of its energy from positive to negative or from negative to positive. When the variation is from positive to negative the maneuver is called a "gravitational capture", to emphasize that the spacecraft was captured by gravitational forces only, with no use of an external force, like the thrust of an engine. The opposite situation, when the energy changes from negative to positive is called a "gravitational escape". In the restricted three-body problem there is no permanent gravitational capture. If the energy changes from positive to negative, it will change back to positive in the future. The mechanism of this capture is very well explained in references 8, 9 and 10.

## ASSUMPTIONS TO STUDY THIS PROBLEM

To study this problem, we made several assumptions. There are:

- i) The true anomaly ( $\gamma$ ) of the secondary body is the parameter used to study the importance of the eccentricity in the problem (see Figure 1);
- ii) The motion is planar;
- iii) The starting point of each trajectory is 100 km from the Moon's surface ( $\approx 0.0045$  in canonical units from the center of the smallest primary). The angle  $\alpha$ , from the line joining the two primaries, shown in Figure 1, is used to compute the initial position;
- iv) The magnitude of the initial velocity is calculated from a given value of  $C_3 = v^2 - 2\mu/r_2$ , where  $v$  is the velocity of the massless body relative to the smallest primary. The direction of the velocity is assumed to be perpendicular to the line joining the smallest primary to the massless body in a counter-clock-wise direction;
- v) The escape occurs when the spacecraft reaches a distance of 100.000 km (0.26 in canonical units) from the center of the smallest primary in a time shorter than 50 days ( $\approx 12$  in canonical units)<sup>10</sup>;
- vi) For each initial condition, the trajectory were numerically integrated backward in time. Every escape in backward time correspond to a gravitational capture in a forward time.

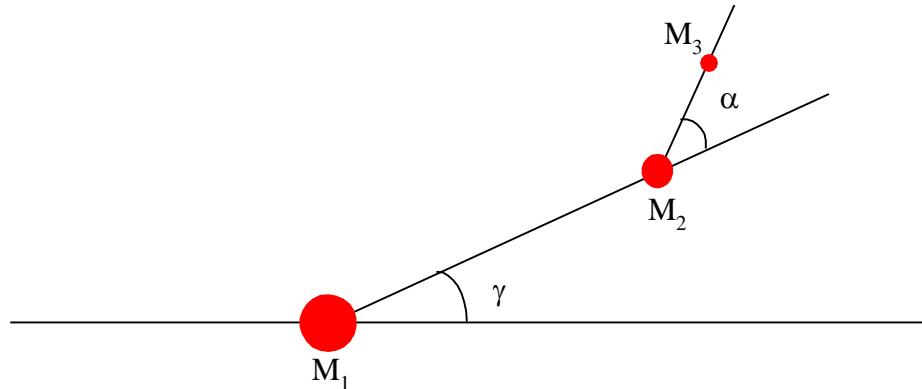


**Figure 1 - Configuration of the Bodies at  $t = 0$  in the Elliptical Restricted Three-Body Problem.**

## SOME RESULTS

As an example of the calculations that we made, we show the results for the cases where the eccentricity of the primaries is kept constant and the true anomaly assumes the values  $0^\circ$ ,  $90^\circ$ ,  $180^\circ$ ,  $270^\circ$ . The Earth-Moon system is used, so the eccentricity is fixed in the value 0.0549. Figure 2 shows the numerical results in plots where the radial variable is the magnitude of  $C_3$  and the angular variable is the angle  $\alpha$ . Figure 3 shows the circular case, for comparison. We can see that the savings are greater where the secondary body is at periaapse ( $\gamma = 0^\circ$ ), what is expected, since the smaller distance between the two primaries increases the effect of the third body (the main cause of the savings). We can also see the regions of maximum and minimum savings. When the Moon is at the perigee, the differences between the circular and elliptic models are very small. These differences are increased for the positions of  $\alpha$  around  $10^\circ$ - $20^\circ$  and  $340^\circ$ - $350^\circ$ . At those points the values of  $C_3$  goes up to  $-0.22$  canonical units for the elliptic case, while for the circular case it stays in  $-0.21$ . Regions around  $70^\circ$ - $80^\circ$  are also of interest.

The fact that the eccentric dynamics has larger savings when compared to the circular one for some points is an important result. The eccentric dynamics represents better the reality, and it is also possible to use it to obtain an extra savings, in the order of 4.76% (from  $-0.21$  to  $-0.22$  canonical units).

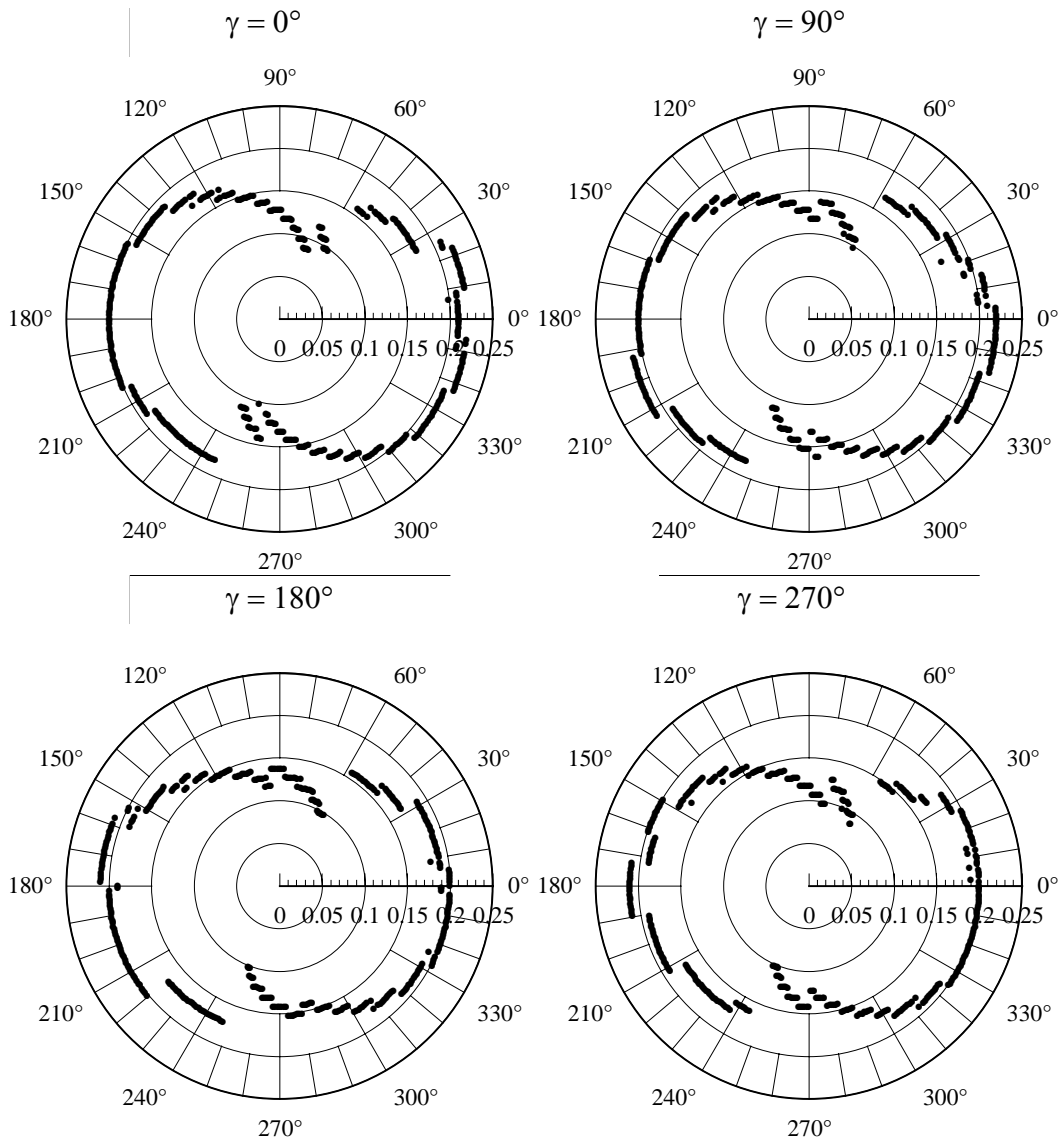


**Figure 2 - Minimum  $C_3$  for the Earth-Moon System with  $\gamma = 0^\circ, 90^\circ, 180^\circ, 270^\circ$ .**

To study in more detail the effect of the initial true anomaly (angle  $\gamma$ ) in the savings of energy, Figure 4 shows the variation of  $C_3$  with  $\gamma$ , when  $\alpha$  is kept fixed.

This figure shows that the conditions in  $\alpha$  are more important than in  $\gamma$  for the values of the eccentricities simulated. When the true anomaly changes, keeping  $\alpha$  constant, the minimum energy is almost the same. In the case where  $\alpha = 0^\circ$ , the perilune are at the apposite side of the Earth, and this geometry allows the minimum values of  $C_3$ .



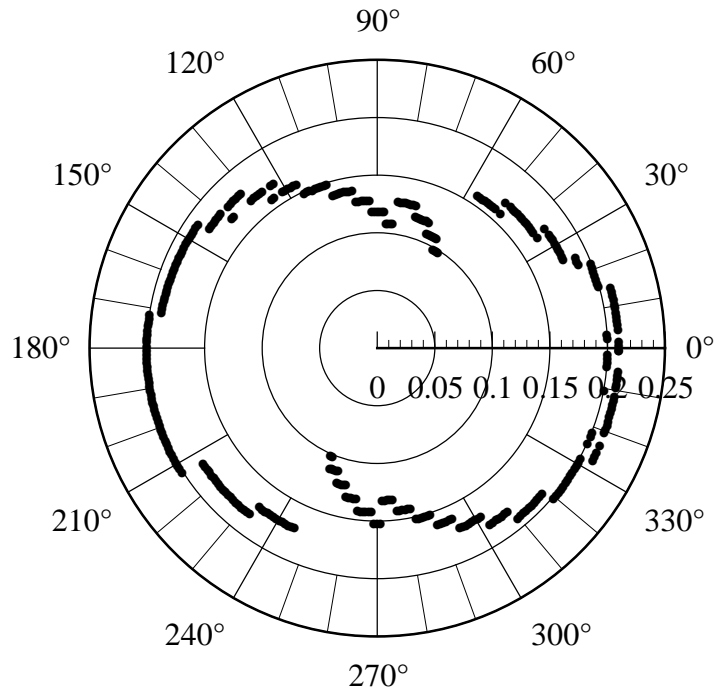


**Figure 3 - Minimum  $C_3$  for the Earth-Moon System Assuming the Circular Case.**

For  $\alpha = 180^\circ$  the minimum energy does not reach levels of energy as low as for the case  $\alpha = 0^\circ$ , but it shows regularity and levels of energy lower than in the cases  $\alpha = 90^\circ$  and  $\alpha = 270^\circ$ . In realistic cases, it is possible to make the transfers when  $\gamma = 0^\circ$ , since there are disadvantages in terms of the potential savings in the cases  $\gamma \neq 0^\circ$ .

Then, some hypothetical systems are studied, with the goal of having more details about the effect of the eccentricity in this problem. Figure 5 shows results when  $\mu = 0.01$ , and the eccentricities of the primaries are 0.0, 0.2, 0.4 and 0.8. The true anomaly assume the values  $0^\circ, 90^\circ, 180^\circ, 270^\circ$  for every value of the eccentricity. In this figure, the magnitude of  $C_3$  in canonical units is the radial variable and the angle  $\alpha$  is the angular variable. The eccentricity is 0.0 for the first plot, 0.2 for the second, 0.4 for the third and 0.8 for the fourth one. It is clear that the lowest level of energy appears when the smaller primary is at periaapse ( $\gamma = 0^\circ$ ) and the worst results appear when it is at the apoapses ( $\gamma = 180^\circ$ ). When  $\gamma = 90^\circ$  and  $\gamma = 270^\circ$  there are intermediate results. This is expected, because the smaller distance between the primaries increase the third body perturbation, that is the main cause of the reduction of energy. From those results it is also possible to conclude that, by increasing the eccentricity, there is an increase in the differences of the level of energy for the families  $\gamma = 0^\circ, 90^\circ, 180^\circ, 270^\circ$  (those families appears with more difference from each other). It is also possible to conclude that the increase of the eccentricity makes the levels of savings to increase. The radial scales goes from 0.2 (for  $e = 0.0$ ) to 0.8 (for  $e = 0.8$ ). Those figures also show the importance

of the choice of the angle  $\alpha$ . The differences in the magnitude of  $C_3$  obtained by different values of this parameter are very large.

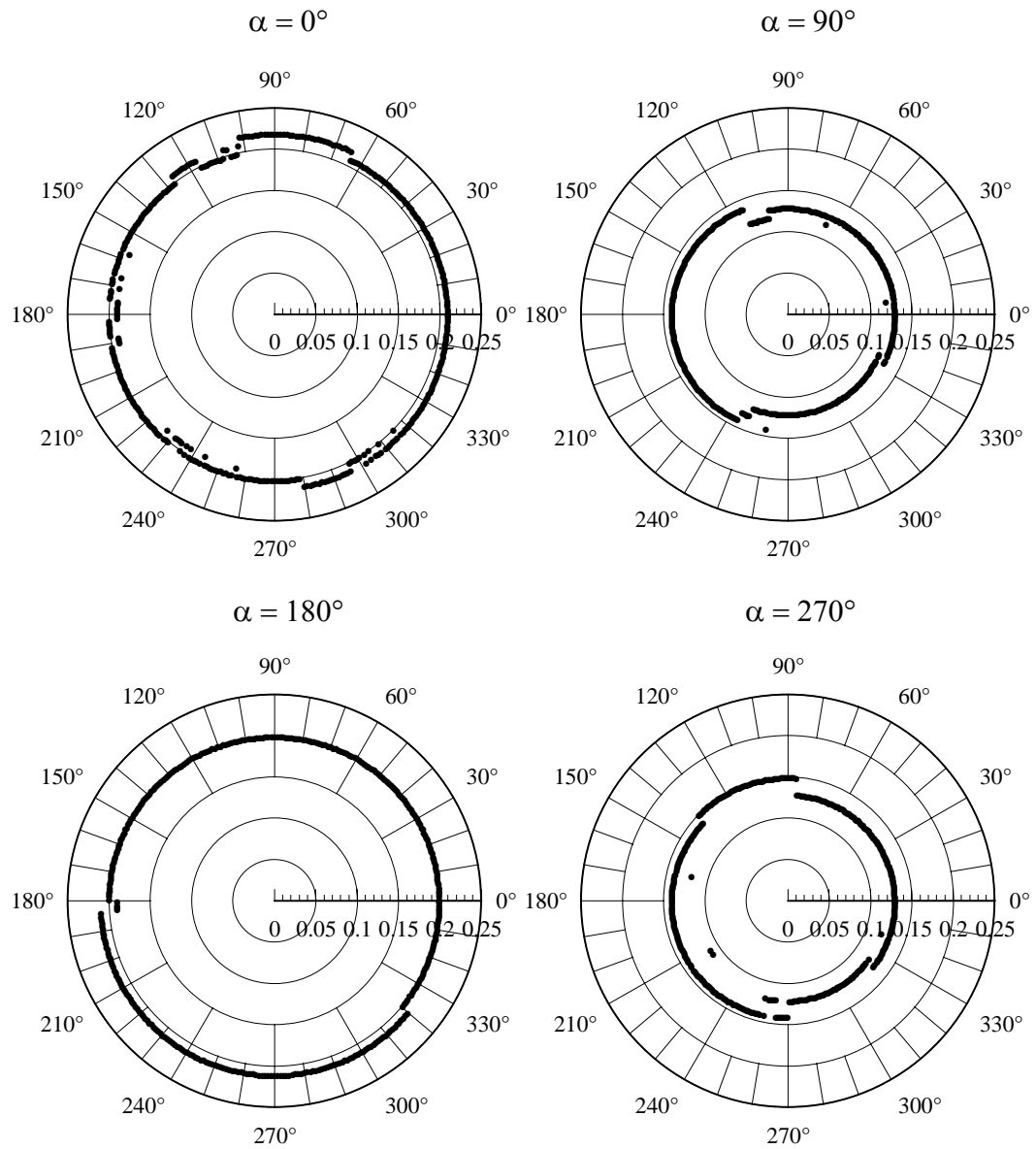


**Figure 4 – Minimum Value of  $C_3$  vs.  $\gamma$  for  $\alpha$  Constant.**

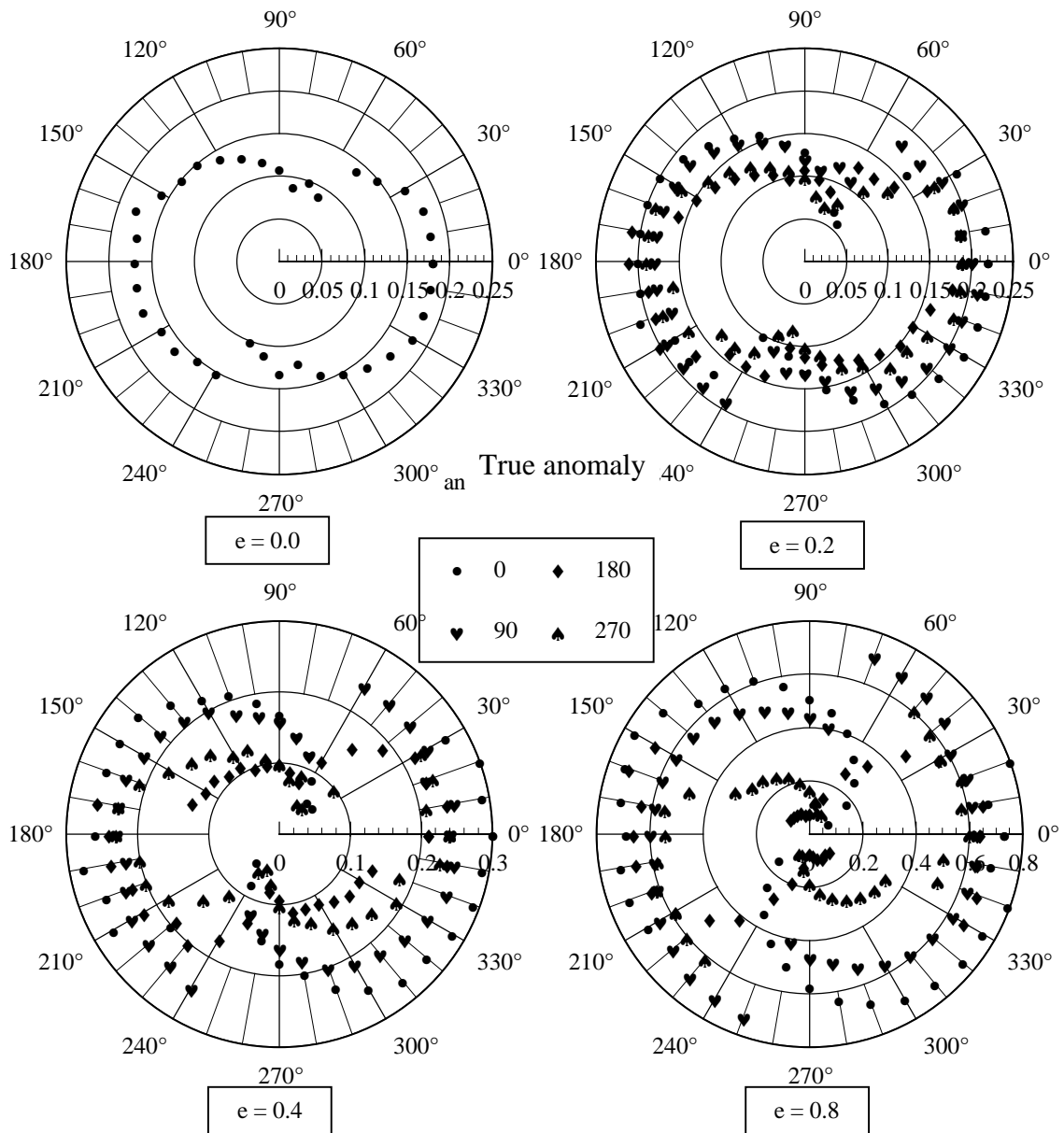


**Figure 5 – Minimum  $C_3$  for  $\mu = 0.01$  and Several Values of the Eccentricity.**

### **EFFECTS OF THE ECCENTRICITY IN THE TIME REQUIRED FOR THE CAPTURE**

For this analysis, the energy  $C_3 = -0.14$  was chosen and fixed. Two situations were studied. In the first one the eccentricity was fixed in 0.4 and the true anomaly varied from  $0^\circ$  to  $270^\circ$  in steps of  $90^\circ$ . These results are shown in Figure 6. In this figure the radial variable is the time of capture in canonical units and the angular variable is the

angle  $\alpha$ . There are four positions for the Moon, where  $\gamma = 0^\circ$  is the position closest to the Earth and  $\gamma = 180^\circ$  is the position with more distance from the Earth. Each point corresponds to one trajectory.

After that, the true anomaly was fixed in  $0^\circ$  and the eccentricity was varied to assume the values 0.0, 0.2, 0.4 e 0.8. These results are shown in Figure 7. Those systems of primaries are similar to the Earth-Moon system, with the eccentricities increased to emphasize the results.

The plots show the existence of two families of trajectories. There are large variations in the time required for the capture, depending on the initial value of the angle  $\alpha$ . This fact shows the importance of this study, because you can get shorter times for the transfer for a fixed value of the energy savings.

Looking at the plots for  $\gamma = 0^\circ$  and  $\gamma = 90^\circ$ , in Figure 6, the change in the results are small, because the majority of the captures has a time smaller than two canonical units. Looking at the case  $\gamma = 180^\circ$ , it is possible to see larger changes in the plots. Two new families of trajectories appears and the majority of them have times of capture between two and four canonical units of time. The largest distance between the two primaries in this geometry reduces the gravitational perturbation and increases the time to complete the capture. The results for  $\gamma = 270^\circ$  shows the return of the two characteristic families. Larger values for the time of capture, when compared to the case  $\gamma = 0^\circ$ , still appears and the number of trajectories that do not belong to the family increases.

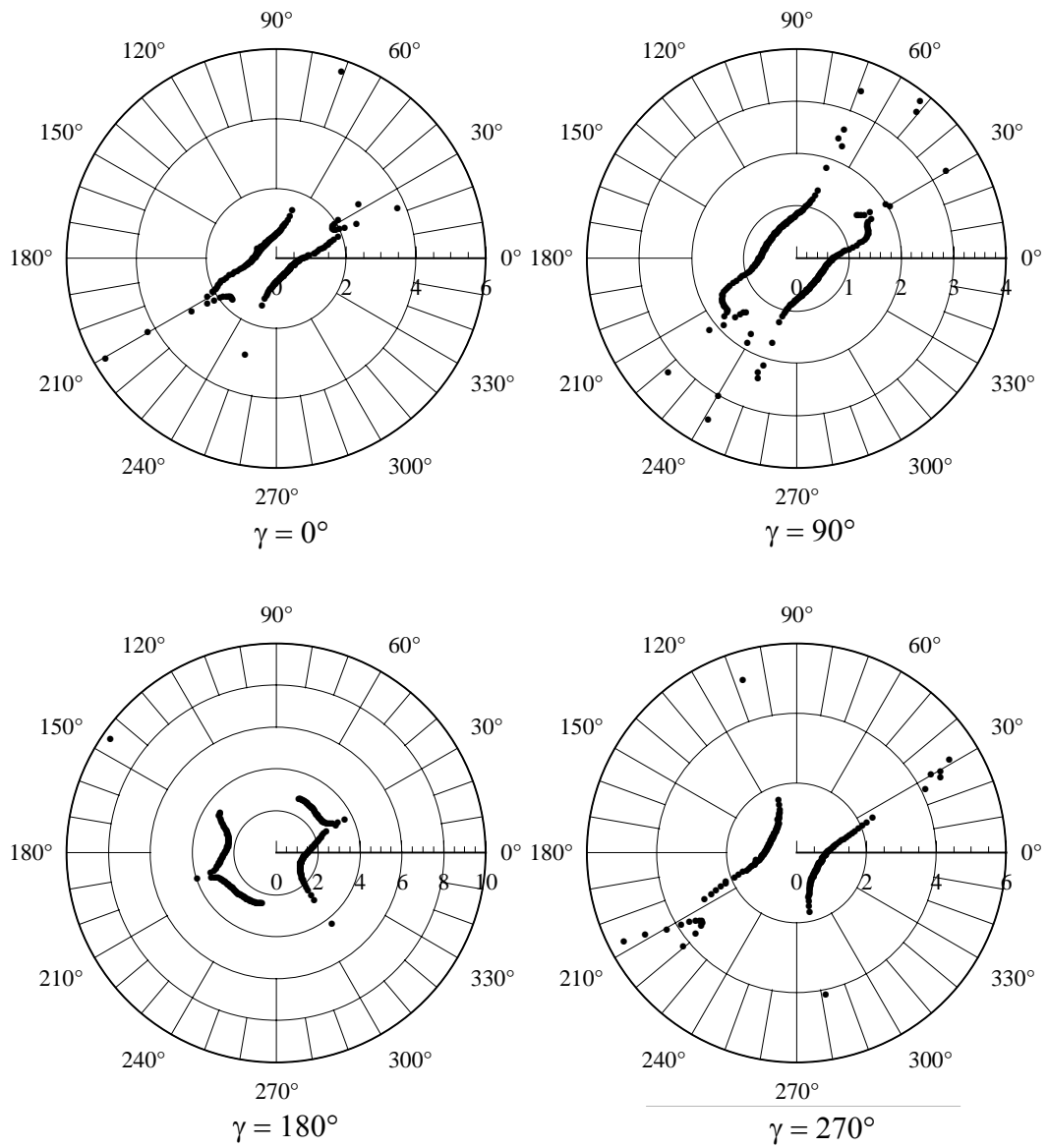


**Figure 6 – Times for the Capture for Eccentricity of 0.4.**

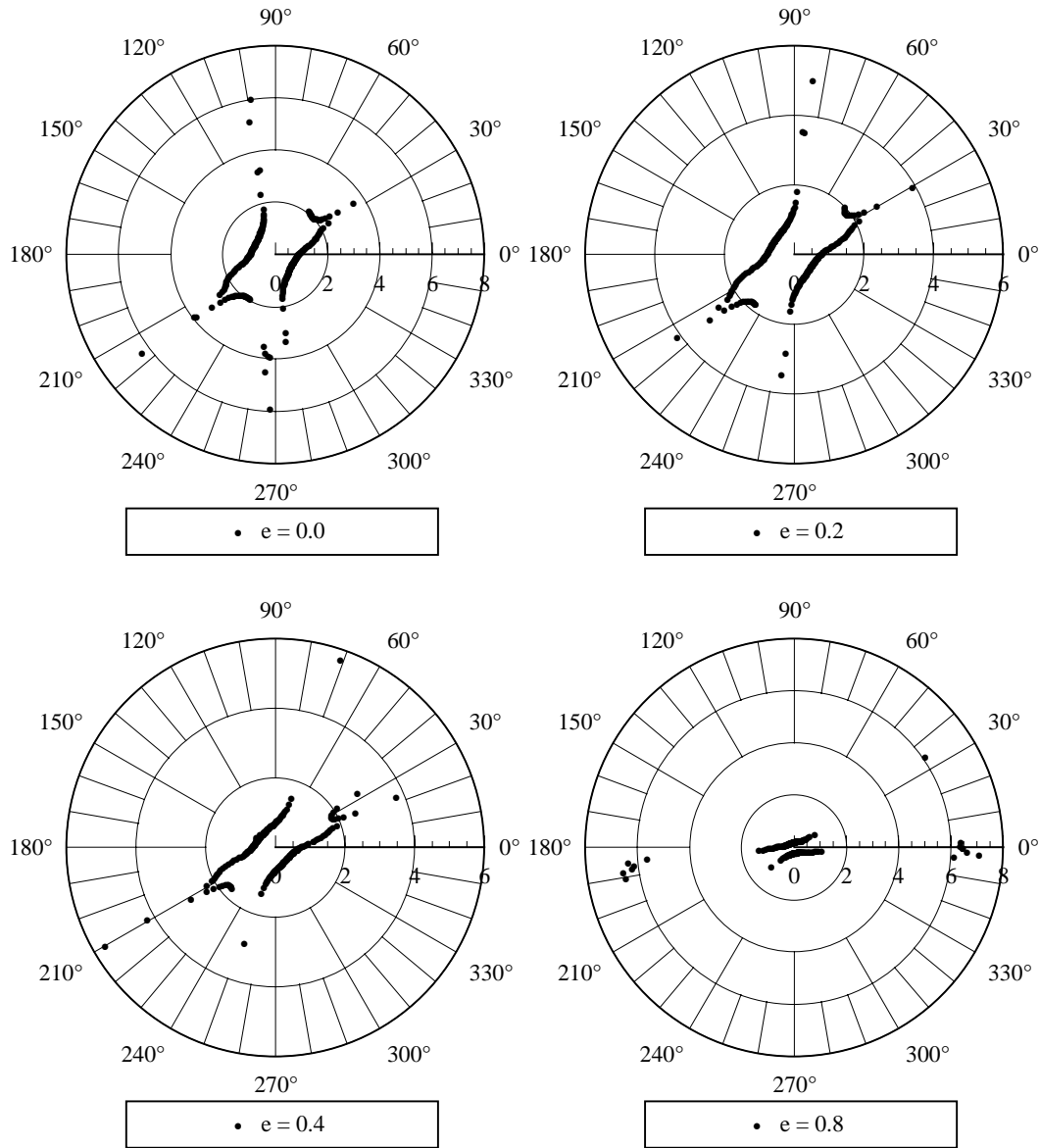


**Figure 7 – Times for the Capture for  $\gamma = 0^\circ$ .**

Figure 7 shows the effect of the eccentricity in the time for the capture when  $\gamma = 0^\circ$  and the eccentricity is varied. In this figure, the radial variable is the time of capture in canonical units and the angular variable is the angle  $\alpha$ . Every point represents one trajectory. The characteristic of the problem of having two families is still valid here, this time for all the plots showed.

Those studies show that there is a measurable effect of the increase of the eccentricity for a fixed value of the true anomaly. In general, there is a tendency to

reduce the time of capture with the increase of the eccentricity. This is also explained by the reduction of the distance between the primaries, since the positions studied is held constant at the periapses. Strong effects appears for large values of the eccentricity (like in  $e = 0.8$ ), where the two families rotate in the clock-wise direction, staying almost horizontal. This means that the value of  $\alpha$  that allow minimum and maximum times of capture changes. These results can be used in optimization problems, like the ones shown below.

## OPTIMIZATION PROBLEMS

Several optimization problems can be solved using the results available in this research. Two of them are shown below.

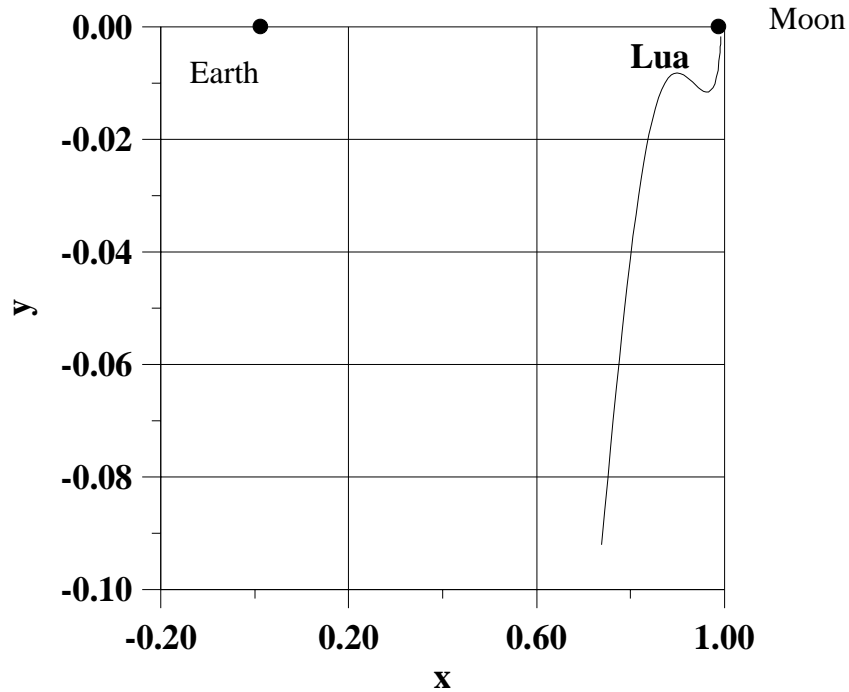
Problem 1: Suppose that it is necessary to build a trajectory that ends in gravitational capture in a given system of primaries and for a fixed value of  $r_p$ . Assuming that  $\mu = 0.0121506683$  (Earth-Moon system), it is desired that this trajectory has the minimum possible time of flight, but with  $C_3 = -0.14$  and  $r_p = 0.004781477$ . Figures 6 and 7 are used to solve this problem. This problem is solved for the eccentricities  $e = 0.0, 0.2, 0.4$  and  $0.8$ . The values for the true anomaly are  $\gamma = 0^\circ, 90^\circ, 180^\circ$  and  $270^\circ$ . The results are shown in Table 1. It includes the angle  $\alpha$  and the time of capture. The savings in  $\Delta V$  obtained is  $0.031296$  canonical units for all the cases, since  $C_3$  is constant.

TABLE 1 – SOLUTIONS FOR PROBLEM 1

$e \backslash \gamma$	$0^\circ$	$90^\circ$	$180^\circ$	$270^\circ$
0	$\alpha = 338^\circ$ $t = 0.7482$	---	---	---
0.2	$\alpha = 311^\circ$ $t = 0.6033$	$335^\circ$ 0.6576	$333^\circ$ 0.9452	$331^\circ$ 0.7656
0.4	$\alpha = 325^\circ$ $t = 0.4556$	$312^\circ$ 0.5402	$354^\circ$ 1.3657	$330^\circ$ 0.7016
0.8	$\alpha = 292^\circ$ $t = 0.1735$	$281^\circ$ 0.1797	$315^\circ$ 2.6443	$330^\circ$ 0.3882

The results are in agreement with the general rule that says that, when getting the primaries closer, the perturbation is larger and the time for the capture is smaller. For a fixed value of the eccentricity, the times are smaller for  $\gamma = 0^\circ$  and larger for  $\gamma = 180^\circ$ . For a fixed value of the true anomaly, the time decrease with the increase of the eccentricity for  $\gamma = 0^\circ$  and it increases when  $\gamma = 180^\circ$ . This means that the differences between the times of capture for different locations of the primaries increase with the eccentricity. The general conclusion is that, taking into account the effects of the eccentricity of the primaries, it is possible to design a trajectory the has the minimum

time of capture. The regions of values of  $\alpha$  does not change much, and the solutions are around  $\alpha = 300^\circ \pm 30^\circ$ . Figure 8 shows the trajectory of a space vehicle for the circular solution, as seen in the rotating frame.



**Figure 8 – Trajectory of Problem 1.**

This type of problem can be solved for different values of  $\mu$ ,  $r_p$ ,  $C_3$ , etc. Similar problems with more degrees of freedom (like free  $r_p$ ) can also be solved with the same technique.

Problem 2: Another variant of optimization problems that can be solved with the data shown here, is the problem of searching a gravitational capture trajectory that has a maximum savings subject to constraints in time, like a maximum time allowed for the maneuver. Figures 6 and 7 are also used to solve this problem. Assume that the Earth-Moon system is used and the value of  $r_p = 0.004781477$  is required, together with the time limit of 0.8 canonical units of time for the maneuver. Again, four possibilities for the eccentricities and for the true anomaly are used. Table 2 shows the results. Compared with the circular solution, it is clear that for a fixed value of the eccentricity,  $C_3$  reaches a minimum for  $\gamma = 0^\circ$  and a maximum for  $\gamma = 180^\circ$ .

Then, the maximum savings for a problem with an upper limit of time is reached for the position  $\gamma = 0^\circ$ . It is also noted that  $C_3$  decreases with the increase of the eccentricity for  $\gamma = 0^\circ$  and that it increases when  $\gamma = 180^\circ$ .



Then, the differences in energy for several final conditions of a specific trajectory increase with the increase of the eccentricity of this trajectory. The general conclusion is that, when we take into account the eccentricity of the primaries, it is possible to design a maneuver with maximum savings for a given time limit for the capture. The region of  $\alpha$  that solves this problem is around  $330^\circ \pm 15^\circ$ . Figure 9 shows the trajectory of a spacecraft for the solution of the circular case, as seen from the rotating system. Solutions for other cases can be obtained by solving a particular problem or interpolating the tables available.

TABLE 2 – SOLUTIONS FOR PROBLEM 2

$e \setminus \gamma$	$0^\circ$	$90^\circ$	$180^\circ$	$270^\circ$
0	$C_3 = -0.15$ $\alpha = 328^\circ$	---	---	---
0.2	$C_3 = -0.19$ $\alpha = 338^\circ$	-0.17 $321^\circ$	-0.11 $346^\circ$	-0.14 $331^\circ$
0.4	$C_3 = -0.28$ $\alpha = 328^\circ$	-0.24 $342^\circ$	-0.09 $328^\circ$	-0.16 $330^\circ$
0.8	$C_3 = -0.85$ $\alpha = 328^\circ$	-0.71 $333^\circ$	-0.07 $346^\circ$	-0.34 $330^\circ$

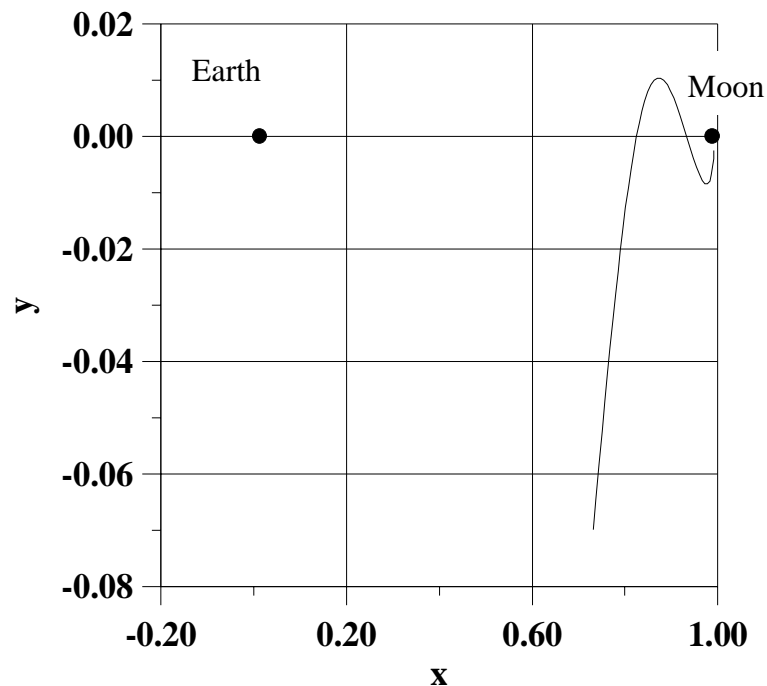


Fig. 9 – Trajectory for Problem 2.

## CONCLUSIONS

We developed a numerical algorithm to study the problem of gravitational capture in the elliptical restricted three-body problem. The effect of the true anomaly for a fixed eccentricity and the effect of the eccentricity for a fixed true anomaly were studied.

From the results available, it is possible to conclude that the elliptic restricted three-body problem has some differences in the results, when compared with the circular case. These differences can be used in real missions to obtain some extra savings in fuel or in time for the maneuver. Figure 5 showed the locations and the magnitude of the differences between the two mathematical models and can be used to find optimal points for the maneuver.

The main effect of the eccentricity is to decrease the two-body energy. Another important effect is that, if  $C_3$  is hold fixed, the time for the capture is reduced when we increase the eccentricity.

Regarding the true anomaly, the periapsis ( $\gamma = 0^\circ$ ) is the best location for the gravitational capture, because it has the larger savings in terms of energy and smaller times of capture.

The results showed in this paper also allow us to formulate and solve several practical problems involving optimization of parameters. Two examples were proposed and solved: 1) To find a trajectory that has a fixed energy and the minimum time of capture and; 2) to find one trajectory that has the minimum energy with a limit time for the capture. Both solutions were shown in details.

## ACKNOWLEDGMENTS

The author is grateful to the Foundation to Support Research in the São Paulo State (FAPESP) for the research grant received under Contract 03/03262-4 and to CNPq (National Council for Scientific and Technological Development) - Brazil for the contract 300828/2003-9.

## REFERENCES

<sup>1</sup>E.A. Belbruno, "Lunar Capture Orbits, a Method of Constructing Earth Moon Trajectories and the Lunar Gas Mission", *AIAA-87-1054*. In: *19th AIAA/DGLR/JSASS International Electric Propulsion Conference*, Colorado Springs, Colorado, May 1987.

<sup>2</sup>E.A. Belbruno, "Examples of the Nonlinear Dynamics of Ballistic Capture and Escape in the Earth-Moon System", *AIAA-90-2896. In: AIAA Astrodynamics Conference*, Portland, Oregon, Aug. 1990.

<sup>3</sup>E.A. Belbruno, "Ballistic Lunar Capture Transfer Using the Fuzzy Boundary and Solar Perturbations: a Survey", *In: Proceedings for the International Congress of SETI Sail and Astrodynamics*, Turin, Italy, 1992.

<sup>4</sup>V. Krish: "An Investigation Into Critical Aspects of a New Form of Low Energy Lunar Transfer, the Belbruno-Miller Trajectories", *Master's Dissertation, Massachusetts Institute of Technology*, Cambridge, MA, Dec1991.

<sup>5</sup>V. Krish, E.A. Belbruno, W.M. Hollister, "An Investigation Into Critical Aspects of a New Form of Low Energy Lunar Transfer, the Belbruno-Miller Trajectories", *AIAA paper 92-4581-CP*, 1992.

<sup>6</sup>J.K. Miller, E.A. Belbruno, "A Method for the Construction of a Lunar Transfer Trajectory Using Ballistic Capture", *AAS-91-100. In: AAS/AIAA Space Flight Mechanics Meeting*, Houston, Texas, Feb. 1991.

<sup>7</sup>E.A. Belbruno, J.K. Miller: "A Ballistic Lunar Capture for the Lunar Observer", *Jet Propulsion Laboratory, JPL IOM 312/90.4-1752, Internal Document*, Pasadena, CA, Aug. 1990.

<sup>8</sup>H. Yamakawa, J. Kawaguchi, N. Ishii, H. Matsuo, "A Numerical Study of Gravitational Capture Orbit in Earth-Moon System", *AAS paper 92-186, AAS/AIAA Spaceflight Mechanics Meeting*, Colorado Springs, Colorado, 1992.

<sup>9</sup>H. Yamakawa, J. Kawaguchi, N. Ishii, H. Matsuo, "On Earth-Moon transfer trajectory with gravitational capture", *AAS paper 93-633, AAS/AIAA Astrodynamics Specialist Conference*, Victoria, CA, 1993.

<sup>10</sup>H. Yamakawa, 1992, On Earth-Moon Transfer Trajectory with Gravitational Capture. *Ph.D. Dissertation*, University of Tokyo.

<sup>11</sup>E.A. Belbruno, J.K. Miller: "A Ballistic Lunar Capture Trajectory for Japanese Spacecraft Hiten", *Jet Propulsion Lab., JPL IOM 312/90.4-1731, Internal Document*, Pasadena, CA, Jun. 1990.

<sup>12</sup>E. Vieira Neto, and A.F.B.A. Prado, A Study of the Gravitational Capture in the Restricted-Problem. *Proceedings of the "International Symposium on Space Dynamics"* pg. 613-622. Toulouse, France, 19-23/June/1995.

<sup>13</sup>E. Vieira Neto, and A.F.B.A. Prado, 1998, Time-of-Flight Analyses for the Gravitational Capture Maneuver. *Journal of Guidance, Control and Dynamics*, Vol. 21, No. 1, pp. 122-126.

<sup>14</sup>J.M. Bailey: "Jupiter: Its Captured Satellites", *Science*, pp. 812-813, Vol. 173, 1971.

<sup>15</sup>J.M. Bailey: "Origin of the Outer Satellites of Jupiter", *Journal of Geophysical Research*, Vol. 76, No. 32, pp. 7827-7832, 1971.

<sup>16</sup>J.M. Bailey: "Studies on Planetary Satellites: Satellite Capture in the Three-Body Elliptical Problem", *The Astronomical Journal*, Vol. 77, No. 2, pp. 177-182I, 1972.

<sup>17</sup>T.A. Heppenheimer: "On the Presumed Capture Origin of Jupiter's Outer Satellites", *Icarus*, Vol. 24, pp. 172-180, 1975.

<sup>18</sup>Szebehely, V.G., "Theory of orbits", *Academic Press*, New York, 1967.